Surface Acoustic Wave Sensors using Nanocrystalline Palladium for Hydrogen Gas Detection

Amol V. Chaudhari, Stefan Cular, Deepak Srinivasagupta, Venkat R. Bhethanabotla[1] and Babu Joseph
Sensors Research Laboratory, Department of Chemical Engineering, University of South Florida, 4202 E. Fowler Ave., ENB 118, Tampa, FL 33620

ABSTRACT

This paper addresses the development of a new gas sensor using surface acoustic wave (SAW) technology. SAW sensors detect the change in mass, modulus, and conductivity of a sensing layer material via absorption or adsorption of an analyte. The advantages of SAW sensors include low cost, small size, high sensitivity, and the possibility of being interrogated wirelessly.

We investigated the use of nanocrystalline palladium as sensing material for improved performance. We also investigated SAW fabrication for radio frequency (RF) range operation where high signal-to-noise ratios can be achieved. A test-bed consisting of a gas dilution system, a temperature-controlled test cell, a network analyzer, and computer-based measurement system was used for evaluating the performance of SAW gas sensors at very low concentrations. Both single and dual delay line SAW devices were fabricated by means of photolithography on a lithium niobate substrate. Tests have been carried out to determine response speed, resolution, reproducibility, and linear characteristics, over a range of analyte concentrations. Future work involves extending these techniques to other sensing materials-analyte combinations.

KEY WORDS

Surface Acoustic Wave sensor, Hydrogen Gas Sensor, Nanocrystalline Palladium

INTRODUCTION

Today, hydrogen is an important industrial chemical. Hydrogen is used as a feedstock in several well-established industries such as chemical, food, metallurgical, electronic, and others, and therefore a limited production, distribution and usage network already exists. Furthermore, prototype hydrogen-fueled automobiles are already on the road.

However, the increasing use of hydrogen gas should not be considered as one without disadvantages. In fact, a number of problems arise involving the storage of this gas. A hydrogen leak in large quantities should be avoided because hydrogen, when mixed with air in the ratio of 4.65-93.9 vol % is explosive (A. Katsuki et al., 1998). Hence, it is important to develop highly sensitive hydrogen detectors to prevent accidents due to its leakage, thus, saving lives and infrastructure. Such detectors should allow continuous monitoring of the concentration of the gas in the environment in a quantitative and selective way.

The majority of the hydrogen sensors use thin palladium films as sensing material because of their well-known absorption properties relative to hydrogen. Surface acoustic wave (SAW) sensors

[1] Corresponding author email: venkat@eng.usf.edu

use a piezoelectric substrate on which surface waves are induced by an alternating electric source. When an active sensing material is placed in the propagation path of these waves, the wave properties are modified because of the interaction of active material with the analyte. The SAW hydrogen sensors that we use have a thin film coating of palladium, which has a well-known affinity for hydrogen (Lewis, 1967). To enhance the response of the SAW sensor, a thin film of metal free phthalocyanine is laid underneath the palladium film (Jakubik, 2002).

Any changes in the physical or chemical properties of a sensing layer placed on a piezoelectric surface can affect SAW propagation. However, from the practical point of view for rigid metal and semi-conducting films such as in this application, only the following two effects are potentially significant, namely, mass loading effect and acousto-electric effect, i.e. the change of its electrical conductivity, which causes a significant change of the velocity and attenuation of SAW (Ballantine et al., 1997). These are explained in the following sections.

BACKGROUND

As the acoustic wave propagates through or on the surface of the material, any changes to the characteristics of the path affect the velocity and/or the amplitude of the wave. Changes in the velocity can be monitored by measuring the frequency change and then be correlated with the physical quantity that is being measured (Ballantine et al., 1997). The generation of the SAW waves is achieved by application of alternating voltage to a metal film inter-digital transducer (IDT) deposited on the surface of a piezoelectric substrate. Two IDTs are required in the basic SAW device configuration sketched in Figure 1. One of these acts as the device input and converts signal voltage variations into mechanical acoustic waves. The other IDT is employed as an output receiver to convert mechanical SAW vibrations back into output voltages. This kind of an arrangement is also referred as a delay line (Campbell, 1989).

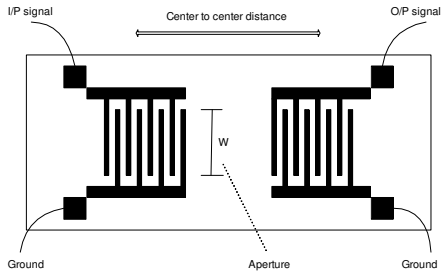

Figure 1. Schematic of typical SAW delay line the electro-acoustic effect.

The nature of the device mostly depends on the properties of the piezoelectric materials such as wave velocity v_0 and electromechanical coupling coefficient K^2.

SAW SENSOR MODEL

The design and simulation of a surface acoustic wave (SAW) sensor follows from the equations of the piezo-electric effect, a model of formation of the surface Raleigh waves, and

A SAW device is fundamentally a band pass filter. To design a SAW device or filter with a given resonant frequency f_0 and fractional bandwidth B (measured null to null on either side of the resonant frequency), we make use of the following equations (Campbell et al., 1989):

The acoustic wavelength (λ) with reference to the above nomenclature is:

$$\lambda = \frac{v_0}{f_0} \qquad (1)$$

The width of each finger that produces a synchronous frequency is $\lambda/4$ and the inter-digital spacing measured center-to-center is $\lambda/2$. The number of finger pairs needed to achieve this fractional bandwidth specification is:

$$N_p = \frac{2}{B} \tag{2}$$

For the best response characteristics, the impedance (Z) of the IDT should be matched with the impedance of the measurement system (typically 50 ohm). The IDT behaves as a capacitive system with the total capacitance determined by the number of finger pairs, their spacing, as well as the degree of overlap. The total capacitance required is:

$$C_t = \frac{1}{2\pi f_0 Z} \tag{3}$$

The aperture *W* (overlap between fingers, in length units) is;

$$W = \frac{C_t}{C_0 N_p} \tag{4}$$

The frequency magnitude response of the IDT approximated as the incoherent addition of contributions from individual fingers is:

$$\phi_1(f) = \left| \frac{\sin(X)}{X} \right| \tag{5}$$

where $X = \frac{N_p \pi (f - f_0)}{f_0}$.

When two IDT are in series spaced apart by a delay path of length L as in a SAW device, the path delay affects only the phase delay and not the magnitude response, as the attenuation losses are negligible at low frequencies. The cumulative frequency magnitude response for the SAW is simply the dot product:

$$S_{21}(f) \equiv \phi_1(f).\phi_2(f) \tag{6}$$

Table 1 lists the typical parameters involved in the design of our SAW sensor.

SAW SENSOR RESPONSE

When a thin film of a selective sensing material is deposited on the delay path of the SAW, this affects the propagation of the surface wave on the piezo-electric crystal. In particular, there is an increased propagation time due to the mass loading of the film. This manifests itself as a change in the observed center frequency from the frequency magnitude response.

Table 1. Independent Parameters for SAW Sensor Design.

Parameter	Value
Piezoelectric Crystal Type	Y-cut Z propagation Lithium Niobate
Surface Acoustic Wave Velocity (v_0)	3488 m/s
Center Frequency (f_0)	200 MHz
Design Impedance (Z)	50 ohm
No. of Finger Pairs (N_p) on a single IDT	50
Delay Path Length (L) (in terms of wavelength λ)	300λ
Capacitance/finger pair-length (C_0)	4.6 pF/cm
Normalized surface particle velocity in x-direction ($\frac{v_{x0}^2}{\omega P}$)	0 cm.g
Normalized surface particle velocity in y-direction ($\frac{v_{y0}^2}{\omega P}$)	0.83×10^{-6} cm.g
Normalized surface particle velocity in z-direction ($\frac{v_{z0}^2}{\omega P}$)	0.56×10^{-6} cm.g
Palladium Film Thickness (h)	200 nm
Palladium Bulk Density (ρ_{Pd})	12023 kg/m^3
Palladium Bulk Conductivity (σ_b)	9.5106 x 10^6 m-ohm
Electromechanical coupling coefficient (squared) (K^2)	4.8 %

The incremental center frequency change due to mass loading effect is (Ballantine et al., 1997):

$$\frac{\Delta f_m}{f_0} = \frac{\Delta v_m}{v_0} = -\frac{\omega v_0 \rho_s}{4}\left(\frac{v_{x0}^2}{\omega P} + \frac{v_{y0}^2}{\omega P} + \frac{v_{z0}^2}{\omega P}\right) \tag{7}$$

where ρ_s is the surface mass density of deposited film with adsorbate, v_{x0}, v_{y0}, and v_{z0} are the SAW particle velocities at the surface. The subscript *m* indicates the contribution from the mass loading effect.

In addition, the electric field is also modified by the conductivity of the deposited film, and this is termed as the electro-acoustic effect. The incremental center frequency change due to electro-acoustic effect (Ballantine et al., 1997) is:

$$\frac{\Delta f_{ea}}{f_0} = \frac{\Delta v_{ea}}{v_0} = -\frac{K^2}{2}\frac{\sigma_s^2}{\sigma_s^2 + (v_0 C_0)^2} \tag{8}$$

Here, K^2 is the squared electromechanical coupling coefficient, and σ_s is the sheet conductivity of the film (film thickness times the bulk conductivity). It may be noted that the sheet conductivity depends on adsorbed analyte (hydrogen) concentration. Normally, hydrogen uptake by palladium results in an increased resistivity (or decreased conductivity), as also changes in film dimensions. In particular, the resistivity follows a linear relationship, and peaks at a factor of 1.8 for a limiting atomic ratio of H/Pd in the solid phase of 0.8.

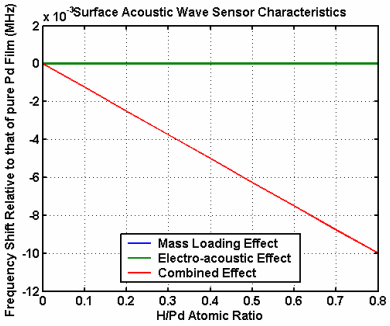

Figure 2. 100 MHz SAW sensor response characteristics

Figure 2 shows the simulated response of a 100 MHz SAW sensor with a delay path length of 300λ. The properties used are that of bulk palladium, with all other relevant parameters from Table 1. The atomic ratio of hydrogen to palladium in the solid phase reaches a maximum of 0.8 at 25 ºC, and this corresponds to a gas phase concentration of 100% hydrogen at 1 atm. pressure. It can be seen that deposition of pure palladium on the delay path essentially eliminates the electro-acoustic response as the conductive palladium film short-circuits the electric field. The overall effect is nothing but the mass loading effect (overlapped in the figure), and this follows a strong and desirable linear behavior. Hence, even though palladium is desirable for the purpose of hydrogen absorption, a film with relatively lower sheet conductivity is desirable for enhancing the electro-acoustic effect. Also, the mass loading response increases quadratically with the resonant frequency of the SAW sensor, as seen in Equation (7). Thus, a higher frequency SAW sensor promises greater sensitivity to the analyte.

EXPERIMENTAL WORK

DEVELOPMENT OF TEST BED - A gas dilution test bed (Figure 3) consisting of arrays of mass-flow controllers to achieve hydrogen concentrations of a few volume percent to ppm range has been designed and fabricated.

An array of five mass flow controllers (MKS 1479A series) is used to mix hydrogen with nitrogen to get the desired concentration. Solenoid valves (ASCO EF8016G1) are used to select the particular gas flow. Both gases go through the mixing chamber to the temperature controlled (using a RM6 LAUDA Brinkmann temperature controller) test cell, where the SAW device is placed. All measurements were done by Agilent 8753ES Vector Network Analyzer. For the dual-delay line configuration, an RF switch (Minicircuits ZASWA-2-509DR) is used to switch between the two delay-lines. Data are transferred to a PC via a data acquisition card (NI PCI-6033E) on a PCI bus.

SAW DEVICE FABRICATION - Single and dual-delay line SAW devices with 50 finger pairs, and a center frequency of 200 MHz were fabricated on Y-Z Lithium Niobate wafers using the standard photolithography processes of etching and lift-off.

The 200 MHz devices were characterized on the Agilent 8753ES Vector Network Analyzer. The S_{21} response (transmission) and S_{11} (reflection) curves are shown in Figures 4 and 5, with a peak close to the designed center frequency of 200 MHz.

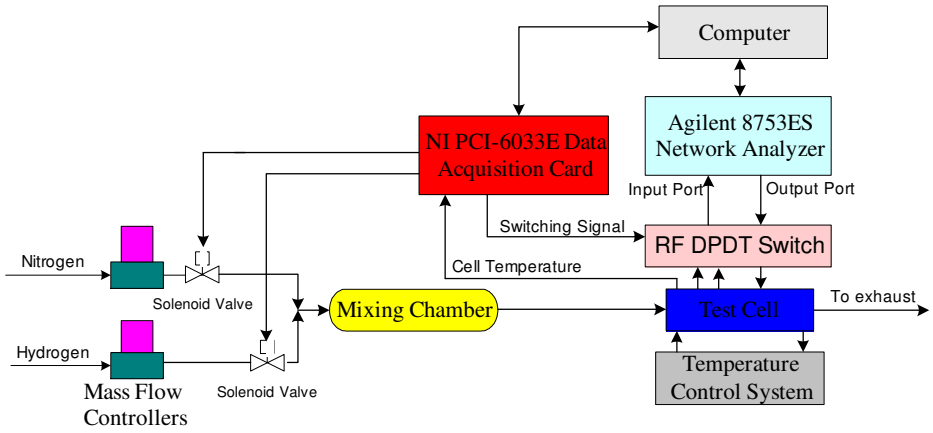

Figure 3. Schematic of gas dilution system

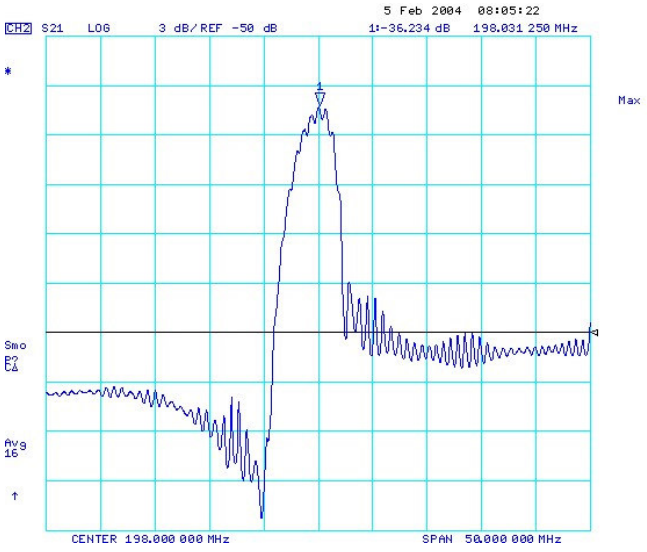

Figure 4. S_{21} (transmission) characteristics of fabricated SAW device

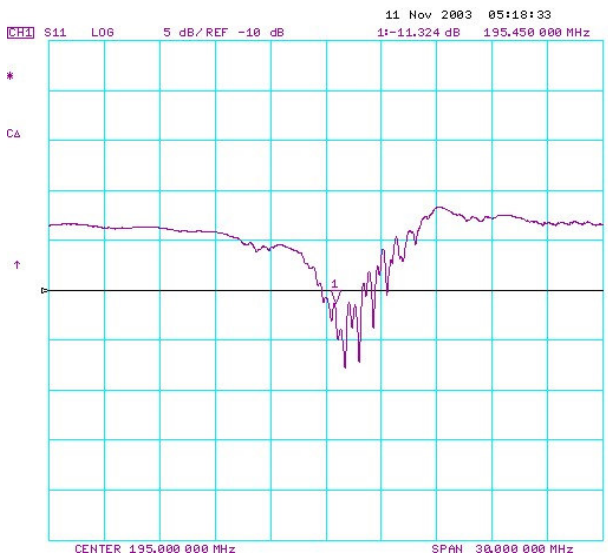

Figure 5. S_{11} (reflection) characteristics of fabricated SAW device

SENSING LAYER SYNTHESIS - After the fabrication of SAW delay lines by above procedures, we put the sensing layer. The sensing layer is deposited on the acoustic path of the devices. The sensing layer consists of a bilayer of metal free phthalocyanine and nanocrystalline palladium.

To deposit the sensing layer a shadow mask made up of aluminum which protects the IDTs was used. We aligned the wafer and mask manually and clamped them together so that only the acoustic path of delay line was exposed. A thin layer of metal free phthalocyanine was coated by using sublimation. The process was carried out in a chamber under a vacuum of around 5 X 10^{-5} Torr. The powdered metal free phthalocyanine was contained in a baffled tantalum box covered with a sieved lid. This specialized boat was required to direct the vapors straight on the wafer which was mounted at a large distance from the source. The thickness of the phthalocyanine layer was 115 nm.

Our preliminary work on Pd films was carried out by sputtering using a multi-gun sputterer at pressures of $1.7x10^{-2}$ torr to $5x10^{-2}$ torr. These films were subjected to rapid thermal annealing at 250 and 350 ˚C. X ray diffraction (XRD) measurements on these films revealed that Pd crystallizes as deposited. XRD profile and AFM picture of the film are shown in Figures 6 and 7. For deposited films, these showed reflections of (111) and (200) peaks, both broadened, indicating nanocrystalline nature of the films. Films subjected to anneal also showed broader peaks, however, a small peak of PdSi emerged due to the reaction between the substrate and the film. From these profiles, a crystallite size of ≈ 30 nm is obtained.

Nanocrystalline thin films are known to have much larger grain boundary volume in the material, leading to increased rates of diffusion of gases. Nanocrystalline thin films of several materials such as Cu, Fe, Mo and Si have been deposited using sputtering (Hernando et al., 2002; Qian et al., 2002; Dahn et al., 2002; Goncalves et al., 2002).

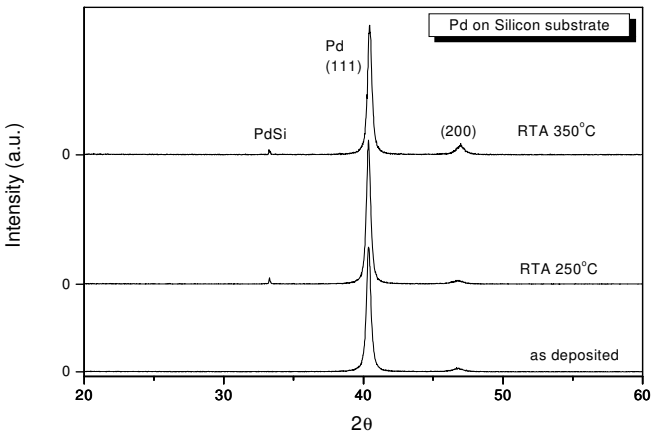

Figure 6. XRD plot of nanocrystalline Pd film

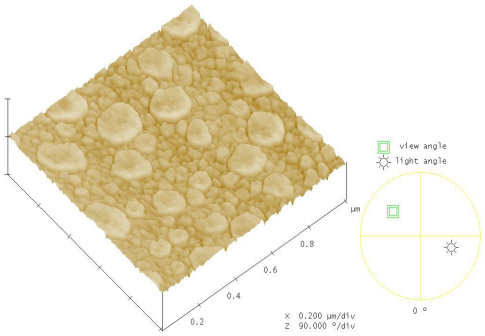

Figure 7. AFM of sputtered nanocrystalline Pd film

SAW DEVICE CHARACTERIZATION -The responses of a 200 MHz SAW sensor coated with 115 nm metal free phthalocyanine and 200 nm nano-crystalline film is shown in Figure 8:

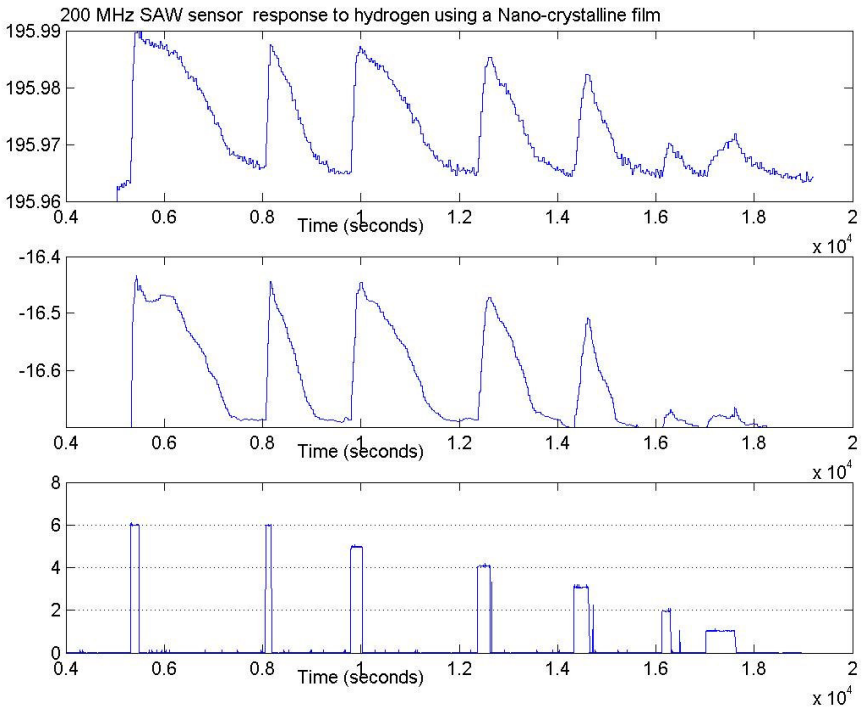

Figure 8. Response of a 200 MHz SAW sensor to hydrogen exposures

The test was carried out at room temperature inside the test cell. The hydrogen was cycled when the maximum center frequency of the device repeated its value for a couple of minutes. As shown in the figures, different concentrations of hydrogen ranging from 1% to 6% were tried. Desired concentration of hydrogen was achieved by mixing it with nitrogen. The flow rate was kept at a total of 1000 SCCM. The observed frequency shifts are large and are in easily detectable ranges using simple and inexpensive electronics.

REPEATABILITY - Repeatability of the sensor was also studied. A pulse of 1% hydrogen was cycled at room temperature. As shown in Figure 9, the sensor shows very good repeatability with a frequency shift of around 40 KHz, when temperature fluctuations are not present. The second peak is widened because the hydrogen pulse duration was longer than the previous one.

TEMPERATURE EFFECTS ON MEASUREMENTS - First of all, the sensor was tested for its temperature stability. A 200 MHz SAW device was put inside the cell. Only temperature was the variable and the rest of the system was kept undisturbed. The temperature was varied from 10 ºC to 50 ºC. As we can see from the graph in Figure 10, the frequency of the SAW device decreases linearly with increasing temperature. The measured temperature coefficient was ~113 ppm/^{0}C.

This graph shows that temperature has a direct effect on the acoustic wave device performance. Changes in temperature produce change in the density of the substrate material which in turn changes the velocity of acoustic waves. In this case, it becomes difficult to operate the sensor in an environment where temperature fluctuates. The heat of adsorption and

absorption of the analyte on to and into the sensing film, respectively, can change the device temperature in most cases.

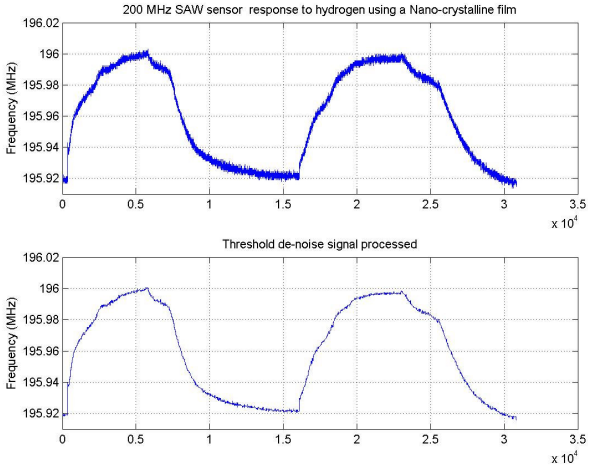

Figure 9 Response of a 200 MHz SAW sensor for 1% Hydrogen cycling

The stringent need of temperature control can be taken care of by using a dual delay line SAW device. In dual delay line configuration, one delay line is coated with the sensing layer while other is left uncoated. If we measure the difference between the two device parameters, all the external effects including temperature will be nullified, except for the very local effects from the heats of adsorption and absorption. One more advantage of this particular set up is that the resultant frequency shifts due to the analyte absorption will be in KHz range and can be measured very easily and economically.

Figure 11 shows the temperature effect on the measurement of dual delay line device by using oscillator circuit. It can be seen that the circuit is stable and has fluctuations in the range of a few Hertz.

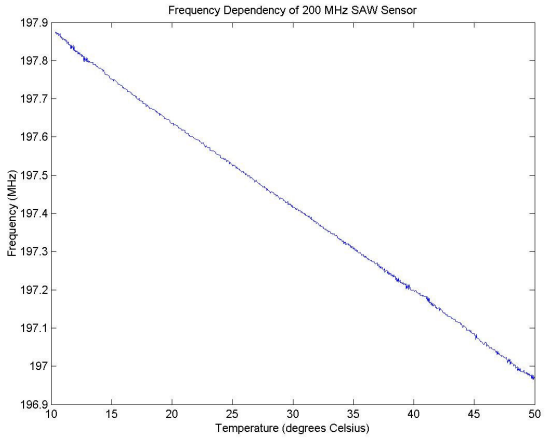

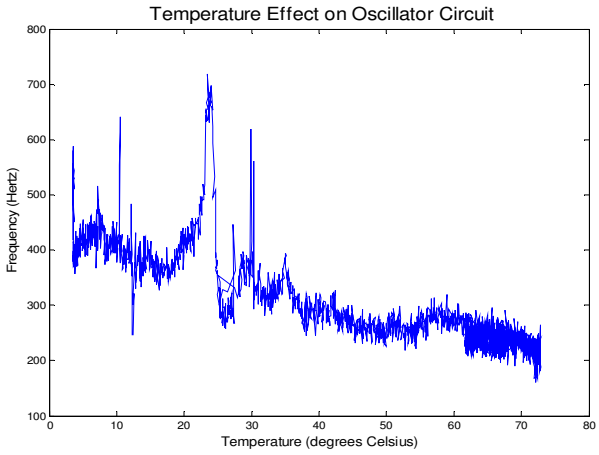

Figure 10. Temperature dependency of 200 MHz SAW sensor.

Figure 11. Temperature effect on oscillator circuit.

DUAL DELAY LINE MEASUREMENTS -A surface acoustic sensor is usually deployed in a field-setting with an oscillator circuit and a frequency counter. Various approaches can be considered for the design of oscillator circuits for SAW sensors (Ballantine et al., 1997, Schmitt et al., 2001) Here, we describe the design of an oscillator circuit to track the resonant frequency of a surface

acoustic wave (SAW) sensor using the linear circuit theory approach. The circuit sets itself into sustained oscillators if it meets the criteria for neutral stability as given by linear dynamic systems theory. Figure 12 below shows a schematic diagram of a typical radio-frequency oscillator circuit. It consists of the following parts: (a) an amplifier, (b) a low-pass filter, (c) a directional coupler, (d) the device under test, i.e., the SAW sensor, (e) a (variable) phase shifter, and (f) an (variable) attenuator. The parts were obtained from Mini-Circuits and were based on the frequency range of operation.

Using the 8753ES vector network analyzer from Agilent, the fabricated SAW sensor was seen to have a loss of around 20 dB at center frequency of 198 MHz, with a (wrapped) phase lag of 180º. The amplifier was seen to have a uniform gain of about 28 dB, nearly independent of frequency. The assembled circuit had a phase shortfall of 15 degrees. No attenuator was found necessary. The final design uses a voltage-controlled variable phase shifter (JSPHS-150 from Mini-Circuits). Figure 13 shows the power spectrum of the oscillator circuit output. A home-built phase shifter was used for this test. As can be seen from the figure, the oscillator circuit is able to lock on to the center frequency of the SAW sensor, and the output from the directional coupler is at a power level of -10 dBm.

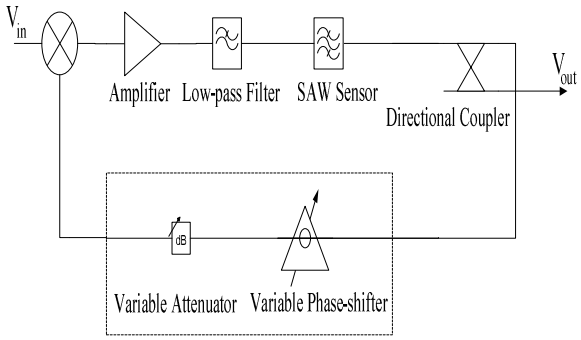

Figure 12. Schematic diagram of oscillator circuit

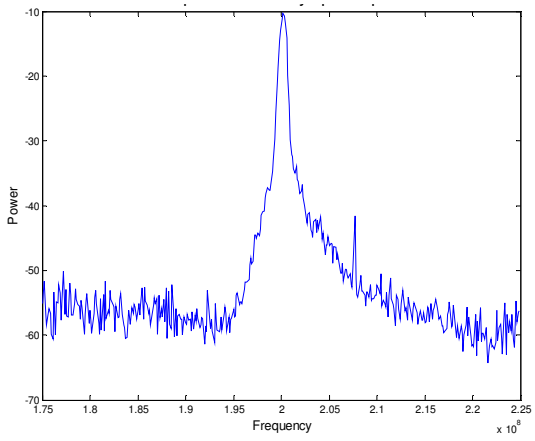

Figure 13. Power spectrum plot of phase-shifted oscillator

In a dual delay line scheme, one SAW delay line is deposited with a sensing layer and acts as the measurement device. The other serves as an environmental reference, primarily, ambient temperature compensation. Both delay lines are identical in design (except for the sensing layer), and their respective center frequencies are tracked by individually oscillator circuits. To achieve ambient temperature adjustment, we need to track the difference between the individual center frequencies. This is achieved by a combination of a square-law radio frequency mixer, and a low pass filter. Dropping the initial phases for mathematical simplicity, if $A_1 \cos(\omega_1 t)$ and $A_2 \cos(\omega_2 t)$ are the outputs from the directional couplers of the two oscillator circuits, we have the non-linear mixer output as:

$$V_{out} = K_1\left[A_1\cos(\omega_1 t) + A_2\cos(\omega_2 t)\right] + K_2\left[A_1\cos(\omega_1 t) + A_2\cos(\omega_2 t)\right]^2 \quad (9)$$

Therefore, the output of the frequency mixer consists of the base frequencies ω_1, and ω_2 as well as the harmonics $2\omega_1$, $2\omega_2$, $\omega_1+\omega_2$, and $\omega_1-\omega_2$. We are interested in the differential frequency $\omega_1-\omega_2$ alone, and this can be obtained by using a simple low pass filtering of the frequency mixer's output. Frequency mixers have been traditionally used in radio receiver circuits, and the inputs are typically not identical.

The frequency mixer we used (Mini-Circuits ZX05-1) consisted of two inputs – a local oscillator (LO) input, and a low-power radio frequency (RF) input. We used an amplifier (ZJL-3G Mini-Circuits) to amplify one of the coupler outputs (~-10 dBm) to meet the input power requirements of the LO input (7 to 10 dBm). The output of the other coupler was fed directly to the RF input. We used SLP-5 from Mini-circuits for the low pass filter stage. This filtered output was then fed to a frequency counter (Agilent 5334B) to record the variations in differential frequency with time.

SUMMARY AND CONCLUSIONS

In this paper, we have described (i) the modeling and design of SAW sensors, (ii) synthesis of nanocrystalline palladium from sputtering processes, (iii) fabrication of SAW devices, (iv) development of a fully instrumented gas dilution test-bed to test these devices, (v) Response of the sensor to different hydrogen concentrations in terms of linearity, repeatability, temperature changes and sensitivity. Future work involves optimization of the sensing layer thickness, using different palladium alloys as sensing layers, using oscillator circuit to test the dual delay line SAW hydrogen sensor and packaging of the sensor for field deployment.

ACKNOWLEDGMENTS

We wish to thank Dr. Senthil N. Sambandam for the thin films deposition, Mr. Kevin Luango for dicing and evaporation operations, and Prof. Horace Gordon for his guidance in designing the oscillator circuit. Funding from NASA through FSEC is gratefully acknowledged.

REFERENCES

1. Ballantine D.S., Jr., White, R.M., Martin, S.J., Ricco, A.J., Frye, G.C., Zellers, E.T., and Wohltjen, H., *Acoustic Wave Sensors: Theory, Design, and Physico-Chemical Applications,* Academic Press, New York, NY, 1997.

2. Campbell, C. *Surface Acoustic Wave Devices and Their Signal Processing Applications*, Academic Press, New York, NY, 1989.

3. Dahn, J.R., Tumer, R.L., Mao, Qu, Dunlop, R.A., George, A.E., Buckett, M.M., McChire, D.J., and Krause, L. J. Structure and properties of sequentially sputtered molybdenum-tin films. Thin Solid Films, 408**,** 111 (2002).

4. Favier, F., Walter, E. C., Zach, M. P., Benter, T., and Penner, R. M., Hydrogen sensors and switches from electrodeposited palladium mesowire arrays. Science (2001), 293(5538), 2227-2231.

5. Goncalves, C., Charvet, S., Zeinert, A., Clin, M., and Zellama, K., Nanocrystalline silicon thin films prepared by radiofrequency magnetron sputtering. Thin Solid Films, 403-404, 91 (2002).

6. Hernando A., Biones, F., Cebollado, A., and Grespo, P., Spin-dependant scattering in nanocrystalline Fe:GMR. Physica B, 322, 318 (2002).

7. Jakubik, W.P., Urbanczyk M.W., Kochowski S., and Bodzenta J., Sensors and Actuators B, **82**, 265 (2002).

8. Katsuki, A., K. Fukui, K., H2 selective gas sensor based on SnO2., Sensors and. Actuators B 52, 30-37, (1998).

9. Lewis, F. A., *Palladium Hydrogen System,* Academic Press, New York, NY, 1967.

10. Qian, L.H., Wang, S.C., Zhao, Y.H., and Lu, K. Microstrain effect on thermal properties of nanocrystalline Cu. Acta Materialia, 50, 3425 (2002).

11. Schmitt, R.F., Allen, J.W., and Wright., Rapid design of SAW oscillator electronics for sensor applications. Sensors and Actuators, B: Chemical 76(1-3) 80-85 (2001).